HHS Public Access

Author manuscript

J Cell Biochem. Author manuscript; available in PMC 2022 April 01.

Published in final edited form as:

J Cell Biochem. 2021 April ; 122(3-4): 413–424. doi:10.1002/jcb.29870.

Identification and initial characterization of a potent inhibitor of ferroptosis

Nishanth Kuganesan[a], **Samkeliso Dlamini**[b], **Jade McDaniel**[b], **Viranga LM Tillekeratne**[b,c], **William R Taylor**[a,c]

[a]Department of Biological Sciences, University of Toledo, 2801 W. Bancroft Street, MS 601, Toledo, OH 43606

[b]Department of Medicinal and Biological Chemistry, University of Toledo, 2801 W. Bancroft Street, MS 601, Toledo, OH 43606

Abstract

Ferroptosis is a form of iron-dependent cell death characterized by elevated lipid peroxides and reactive oxygen species (ROS). Glutathione (GSH) plays an essential role in scavenging ROS to maintain cell viability, and acts as a cofactor of GSH peroxidase 4 (GPX4) that protects lipids from oxidation. We have previously described a novel class of small molecules that induce ferroptosis in certain types of cancer cells. These compounds induce ferroptosis by blocking uptake of cystine required for GSH synthesis. Even though ferroptosis is a well-established form of cell death, signaling pathways that modulate this process are not known. Therefore, we used a panel of growth factors/kinase inhibitors to test effects on ferroptosis induced by our lead compound. We discovered that BMS536924, a dual inhibitor of insulin like growth and insulin receptors, is a potent inhibitor of ferroptosis. Further investigation indicated that the anti-ferroptotic activity of BMS536924 does not lie in its ability to inhibit insulin signal transduction. Instead, we provide evidence that BMS536924 binds iron, an essential co-factor in ferroptosis. Our results suggest caution in interpreting the effects of BMS536924 in investigations of insulin signaling and uncover a novel ferroptosis inhibitor.

Keywords

Insulin; ROS; Iron; Cystine; Cysteine; Xc-

[c]WRT and LMVT should be considered joint senior author. WRT: Tel: (419) 530-1966, william.taylor3@utoledo.edu; LMVT: Tel: (419)-530-1983, ltillek@utnet.utoledo.edu.

Author contributions. NK carried out all biological studies and contributed to writing the manuscript. SD and JM synthesized and purified compounds 1 and 2. VLMT and WRT conceived of the study, directed the research, wrote and edited the manuscript.

Declaration of Interest. WRT and LMVT appear as inventors on patents covering the compounds described in this manuscript and related analogues. Declarations of interest for NK, SD, and JM: none.

Data Accessibility Statement. The data that supports the findings of this study are available in the supplementary material of this article

Introduction

In the last few years, there has been intense focus on a form of reactive oxygen species (ROS)-mediated cell death that occurs when anti-oxidant mechanisms are inhibited, usually with small-molecule inhibitors. This form of cell death, called ferroptosis (Dixon et al., 2012), requires iron to amplify ROS produced through cell-intrinsic pathways that ultimately attack membrane lipids leading to cell lysis. Inducers of ferroptosis have been broadly characterized as having two major intracellular targets. Type I ferroptotic inducers block import of cystine via the Xc- transporter. Cystine, being required to regenerate reduced glutathione, is essential to avoid ferroptosis. However, cystine dependence is cell type specific by mechanisms that are not completely defined. Type II ferroptotic inducers inhibit GPX4, an enzyme that removes toxic lipid peroxides using glutathione as a reducing agent.

We have recently described the design, synthesis and characterization of a new class ferroptotic inducers. We provided several lines of evidence that these molecules function by the Type I mechanism (Fedorka et al., 2018; Taylor et al., 2019). For example, these compounds increase cellular ROS and lipid ROS, while reducing cellular thiols and glutathione as well as blocking glutamate export and cystine import. Cell death is rapid and blocked by anti-oxidants, iron chelators, and an inhibitor of NADPH oxidase. Detailed analysis of at least 20 different normal and cancer cell lines show our compounds attack mesenchymal cells and cancer stem cells preferentially. Our extensive SAR studies encompassing at least 30 analogues have pinpointed essential chemical features required for optimal activity.

Many previous studies have defined important features of ferroptosis including inhibition by iron chelators, ROS scavengers and inhibitors of NADPH oxidases. Ferroptosis is also regulated by various signaling pathways including p53, ataxia telangiectasia mutated (ATM), Sirtuin 1(SIRT1), and HIPPO pathway, among others (Chen et al., 2020; Chu et al., 2019; Venkatesh et al., 2020; W. H. Yang & Chi, 2020; Zhou et al., 2020). Here we describe a potent inhibitor of ferroptosis that was initially characterized as an inhibitor of insulin signaling. We provide evidence that, in the context of ferroptosis, this compound works by chelating iron and not by its effects on insulin signaling. Ferroptosis has multiple important cellular consequences, for example being involved in neuronal death in response to ischemia. There is also a concerted effort to harness ferroptosis as a treatment for cancer. Continued study of novel inducers and inhibitors of ferroptosis will contribute to this goal.

Materials and Methods.

Cell Lines and Culture Conditions.

NCI-H522, HT1080 and MDA MB 231 cell lines were cultured in a humidified atmosphere containing 10% CO_2 in Dulbecco's Modified Eagle's Medium (DMEM; Mediatech, Inc.) supplemented with either 10% fetal bovine serum (FBS; Atlanta Biologicals) or bovine calf serum (RMBIO). In experiments where cells were incubated without cystine, DMEM lacking the amino acid was supplemented with 10% dialyzed FBS (dFBS). dFBS was prepared using dialysis membrane with a 3500 MW cutoff. 50 ml of FBS (Thermofisher) was dialyzed against 1 liter of saline (0.8% NaCl) with 2 changes with 16 and 24 hours

between each change, respectively. dFBS was filtered through a 0.45-micron filter for sterilization. Insulin-like growth factor 1 (IGF1) was obtained from Thermofisher and dissolved in H_2O before use. In order to generate conditioned medium, 2×10^6 NCI-H522 cells were plated on a 10cm plate in 10% FBS in DMEM. Next day, cells were washed three times with phosphate buffered saline (PBS) and media replaced with serum free DMEM. Conditioned media was harvested either 24 or 48 hours later.

Chemicals and cell viability.

All commercially available chemicals were obtained from Cayman Chemicals. Compound **1** was synthesized in-house as we have previously described (Fedorka et al., 2018). In a typical viability assay, 25,000 cells were plated per well of a 24-well plate and drugs added next day. Cells were stained 24–72 hours post treatment with a saturated solution of methylene blue in 50% ethanol. Plates were rinsed with tap water and dried. Dye was dissolved by addition of 0.5 ml 0.1 M HCl in water and then detected using spectrophotometry to measure absorbance at 668 nm. Results are representative of at least two independent experiments. Supplemental Figure 1 shows a comparison of methylene blue assay with MTT assay for cell viability. MTT assay: 12 mM MTT stock solution (10 X) was prepared in 1X PBS. For 24 well plates, at the harvesting time, media was replaced with 300 µl fresh media. Thirty µl of MTT stock solution was added and incubated at 37°C. After 3 hours, equal amount of MTT lysis buffer (0.01N HCl in 10% SDS) was added and incubated for 15 minutes. Finally, absorbance was measured at 540 nm.

Western Blotting.

Cells growing on a 7cm plate were harvested by scraping and lysed in 3 pellet volumes (100–200µl) of RIPA buffer [10 mM Tris (pH 7.4), 150 mM NaCl, 1% NP-40, 1% DOC, 0.1% SDS, 1 mg/ml aprotinin, 2 mg/ml leupeptin, 1 mg/ml pepstatin A, 1 mM DTT, 0.1M phenylmethylsulfonyl fluoride, 1 mM sodium fluoride and 1 mM sodium vanadate]. Lysis was for 20 minutes on ice, followed by removal of insoluble debris by centrifugation at 16,000 g for 20 minutes at 4°C. Equal microgram quantities of total protein for each sample (determined using BCA protein assay kit - Pierce) were separated by sodium dodecyl sulfate-polyacrylamide gel electrophoresis (SDS-PAGE). Gels were transferred to polyvinylidene difluoride membranes (Millipore), which were incubated in blocking buffer (5% (w/v) non-fat dry milk dissolved in PBST [PBS containing 0.05% (v/v) Tween 20]) and probed with antibodies as indicated. For phospho-antibodies, membranes were blocked in bovine serum albumin dissolved in Tris-buffered saline. Uncropped gel images and repeat experiments are in supplemental figures 2–5.

Antibodies were generally diluted in blocking buffer at 1:1000. Primary antibodies recognizing phosho-ERK (Cell Signaling Technology CST #4370), total ERK (Santa Cruz sc #514302) phospho-AKT (CST #4060S), total AKT1 (CST #2938T), ferritin light chain (proteintech #10727–1-AP), Actin (Abcam #3280) and IRP2 (CST #37135) were generally incubated with membranes for 1.5 hour at room temperature (or 4° overnight) once diluted. Signals were detected using horse-radish peroxidase conjugated secondary antibodies (Biorad) diluted 1:10,000 in blocking buffer and enhanced chemiluminescence (Biorad).

Iron Chelation and Radical Scavenging.

To assess potential for iron binding, BMS536924 was dissolved at 100 μM in dimethyl sulfoxide (DMSO) and analyzed by wavelength scanning spectrophotometry. Sample volumes were generally below 10 μl and scans obtained using a nanospec (1 μl/scan). Scans were repeated in the presence of the indicated concentrations of ferrous sulfate. To test intracellular iron binding, we used calcein AM, a fluorescent iron indicator. Fifty thousand NCI-H522 cells were plated in a 24-well plate. Twenty four hours later compounds were added. After another 24 hours, calcein AM was added at 0.5 μM and incubated for 15 min in 37 °C. Then media was replaced with Ham's F12 media and fluorescence images were taken using an EVOS fluorescence microscope. Raw pixel intensities of the images were analyzed using Image J software. In order to test potential radical scavenging activity, DPPH (Cayman Chemicals) was dissolved in methanol at 0.24 mg/ml. Next, trolox or BMS536924 or DMSO were diluted at given concentrations in methanol to 150 μl volume. Later, 50 μl of the DPPH was added to each well of the 96-well plate. After 10 minutes, the absorbance at 517 nm was measured by spectrophotometry with a loss of absorbance indicating radical scavenging activity.

Statistical analysis.

Statistical significance was determined ($p < 0.05$) by student t-test. Measurements of cell viability involved preparation of triplicate samples, used to calculate averages and standard deviations. All cell viability studies were repeated in this manner at least once (total $n \geq 6$). Western blot experiments were carried out in triplicate using three independent cell lysates in some cases run on the same gel. Films were scanned and pixel intensities determined using ImageJ.

Results

Effects of growth factor inhibitors on ferroptosis.

We recently reported a potential anti-cancer agent, compound **1** that induces ferroptotic cell death in certain cell lines (Fedorka et al., 2018; Taylor et al., 2019). Compound **1**, based upon all available evidence, is a novel inhibitor of the Xc- cystine transporter, required to replenish cysteine for glutathione synthesis (Taylor et al., 2019). Surprisingly, we observed that cell death was significantly inhibited when the compound **1** treatment was performed in presence of 10% bovine calf serum (BCS) instead of fetal bovine serum (FBS) using the non-small cell lung cancer cell line NCI H522 (Fig. 1A, B)(Kuganesan, Dlamini, McDaniel, Tillekeratne, & Taylor, 2020). Since growth factors are one of the prime factors in sera, we tested a panel of growth factor receptor inhibitors to determine their effects on ferroptosis. NCI-H522 cells growing in 10% FBS were treated with compound **1** in the presence or absence of the inhibitors. Some of the inhibitors were toxic on their own at the concentrations tested, but only BMS536924, a dual inhibitor of insulin like growth and insulin receptors, rescued compound **1**-induced cell death (Fig. 1C, 2A). In these experiments, cell viability was measured using methylene blue which stains macromolecules. Since ferroptosis results in loss of plasma membrane integrity, methylene blue staining in cultures of adherent cells is lost. We compared methylene blue to the MTT assay which measures cellular reductants resulting from ongoing metabolism. Very similar

values were obtained with both assays when cells were triggered to undergo ferroptosis using compound **1** (Supplemental Figure 1).

BMS536924 blocks ferroptosis.

Ferroptosis can be induced by growing cells in media lacking cystine. This condition leads to depletion of glutathione, accumulation of ROS and peroxidation of membrane lipids (Dixon et al., 2012). BMS536924 rescued cells incubated in cystine-minus medium, however the rescue was not as efficient as in cells exposed to compound **1** (Fig. 2B). Rescue of ferroptosis by BMS536924 was dose-dependent with a maximal protective effect at ~1 μM (Fig. 2C, D). When used at 1 μM, BMS536924 protected NCI-H522 cells from either 5 or 10 μM compound **1** (Fig 2E). Higher concentrations of compound **1** were toxic even in the presence of BMS536924 (Fig 2E). Similarly, BMS536924 protected cells from death induced by RSL3, an inhibitor of the Gpx4 enzyme that is central to detoxification of lipid ROS (W. S. Yang et al., 2014) (Fig. 2F). BMS536924 at 1 μM protected NCI-H522 cells treated with up to 100 nM RSL3 (Fig. 2F). Therefore, BMS536924 protects cells from multiple inducers of ferroptosis.

Serum starvation modulates ferroptotic sensitivity.

Given the lack of ferroptosis when cells are grown in BCS, we decided to investigate the effects of FBS in more detail. Compound **1** was still capable of killing NCI-H522 cells in the absence of serum (Fig. 3A). In this experiment, cells were plated in medium containing 10% FBS. Twenty-four hours later, medium was changed and replaced with serum-free medium. At the same time, compound **1** was added and viability was clearly reduced 24 hours later (Fig 3A). Cell death under these conditions was blocked by either BMS536924, the antioxidant trolox, the lipid ROS scavenger liproxstatin-1, or the iron chelator CPO (Fig. 3A). Thus, compound **1** can induce ferroptosis even in the absence of serum. Next, we tested the effect of extended incubation in serum free medium. NCI-H522 cells were plated in 10% FBS and 24 hours later media replaced with serum-free media. Cells were incubated in serum-free media for 24 hours and then compound **1** was added. Compound **1** showed no evidence of ferroptosis 24 hours later (Fig. 3B). Therefore, serum removal for 24 hours renders cells resistant to compound **1**. We observed very similar results when we tested HT1080 cells instead of NCI-H522. Compound **1** still killed HT1080 cells when serum was removed at the time of compound **1** addition (Fig. 3C) but not if serum was removed for 24 hours before adding compound **1** (Fig. 3D).

In tissue culture studies, serum provides growth factors to modulate cell responses. In natural settings, these factors originate from paracrine or autocrine sources. To test whether autocrine factors might modulate ferroptosis, we tested the effect of conditioned media on this response. NCI-H522 cells were incubated in serum free media for 24 hours to render them resistant to compound **1**. In another plate, NCI-H522 cells were incubated for either 24 or 48 hours in serum free media to create 1 day conditioned media (1d CM) or 2d CM. Adding 1d CM to starved NCI-H522 cells had little effect, however 2d CM significantly increased cell death induced by compound **1** (Fig. 3E, F). These experiments suggest that NCI-H522 may secrete factors that enhance ferroptosis.

Insulin signaling does not affect ferroptosis.

The strong inhibitory effect of BMS536924 on ferroptosis suggested that insulin or insulin like growth factors (IGFs) might modulate ferroptosis. However, compound BMS754807 (Cayman), another dual inhibitor of insulin or IGF1 receptors, had little effect on ferroptosis (our unpublished data). Additionally, NVP-AEW541 (hydrochloride) (Cayman), an IGF1 receptor inhibitor showed no significant effect on ferroptosis (our unpublished data). IGF1 can activate both the insulin receptor and the IGF1 receptor (Denley, Cosgrove, Booker, Wallace, & Forbes, 2005). To directly test if the activity of either of these receptors modulate ferroptosis we added IGF1 to either NCI-H522 or MDA MB 231 cells, a breast cancer cell line that is sensitive to compound **1** (Taylor et al., 2019). Compound **1** killed 76.5% of NCI-H522 and adding IGF1 at 100 ng/ml had no additional effect (Fig. 4A). Similarly, IGF1 did not enhance killing of MDA MB 231 cells by compound **1** (Fig. 4B). In these initial experiments, IGF1 and compound **1** were added to cells in the presence of 10% FBS. However, even when IGF1 was added to MDA MB 231 cells that had been starved in serum-free media for 24 hours, there was no enhancement of compound **1**-induced cell death (Fig. 4C). Our stock of IGF1 was able to induce Akt phosphorylation confirming that the growth factor retained biology activity (Fig. 4D). Furthermore, BMS536924 reduced Akt phosphorylation consistent with its characterization as an inhibitor of insulin signaling.

BMS536924 does not inhibit MEK to block ferroptosis.

BMS536924 inhibits MEK in in vitro assays suggesting one possible relevant off-target effect (Wittman et al., 2005). Related to this is the observation that the MEK inhibitor U0126 blocks ferroptosis (Yagoda et al., 2007). This observation suggests that the Ras-MAPK pathway may enhance ferroptosis. However, the role of MEK in ferroptosis has been called into question given the fact that U0126 can scavenge ROS, and the fact that PD0325901, another MEK inhibitor, does not block ferroptosis (Gao, Monian, Quadri, Ramasamy, & Jiang, 2015). To address effects of BMS536924 on MEK, we measured the effect of BMS536924 on ERK phosphorylation (a MEK substrate) in HT1080 cells harboring activated N-RAS (Brown, Marshall, Pennie, & Hall, 1984). We reasoned that if BMS536924 inhibited ERK phosphorylation in HT1080 cells, this would likely not be due to inhibition of insulin signaling upstream of the constitutive RAS, and more likely due to off-target inhibition of MEK. BMS536924 had no significant effect on ERK phosphorylation in HT1080 cells suggesting that MEK is not a physiological target (Fig. 4E, F). Interestingly, the iron chelator DFO caused a dramatic upregulation of ERK phosphorylation similar to effects previously reported with other iron chelators (Fig. 4E, F)(Lee, Lee, Prywes, & Vulpe, 2015).

BMS536924 is not a free radical scavenger.

Although BMS536924 is a potent inhibitor of ferroptosis, this activity does not appear to be related to its ability to inhibit insulin signaling. Consistent with this idea, we observed that BMS536924 could rapidly block ferroptosis. For example, time-lapse microscopy experiments indicate that ~50% of NCI-H522 cells are dead within 10 hours of treatment with compound **2** (a precursor of compound **1**)(Fig. 1A)(Fedorka et al., 2018). BMS536924 could block killing even when added 8 hours after adding compound **1**, suggesting very fast

kinetics of protection (Fig. 5). It is possible that BMS536924 may rapidly affect a key signal transduction pathway in just a few hours to block ferroptosis. However, partly based on these fast kinetics, we considered that BMS536924 may have a direct effect on key components of the ferroptotic pathway. First, we used the stable radial 2,2-diphenyl-1-(2,4,6-trinitrophenyl)-hydrazyl (DPPH) to test whether BMS536924 might be a free radical scavenger. DPPH is purple in solution until it is reduced by radical scavengers, a process that can be monitored by spectrophotometry. We observed that BMS536924 had minimal effect on DPPH absorbance even up to 100μM, unlike trolox which immediately rendered the DPPH solution colorless (Fig. 6). This suggests that BMS536924 likely does not block ferroptosis by scavenging free radicals.

BMS536924 may function as an iron chelator.

Ferroptosis relies on iron-catalyzed reactions to generate ROS. We tested whether BMS536924 might block ferroptosis by chelating iron. BMS536924 absorbs light with three major peaks (λmax ~223 nm, 236 nm and 353 nm) (Fig. 7A). Adding iron (Ferrous sulfate) both reduced the peak height and shifted the λmax in all three regions of the spectrum (Fig. 7A). These changes are consistent with a direct interaction of BMS536924 with iron under these conditions. To further characterize this interaction, we varied pH by dissolving BMS536924 in potassium phosphate buffer. This buffer system suppressed absorbance at 350 nM, but still facilitated absorbance between 200 to 236 nm (Fig 7B). pH changed the absorbance of BMS536924 alone (Fig. 7C). Also, adding iron further altered absorbance, but only at pH 5.8 and 6.4 (Fig. 7D). Therefore, pH modulates the interaction of iron with BMS536924.

To determine whether BMS536924 might alter free iron in treated cells, we used two approaches. First, we stained cells with the intracellular iron sensor calcein AM. Binding of iron to calcein AM quenches its fluorescence allowing iron chelation activity to be measured as a recovery of fluorescence. BMS536924 significantly increased calcein AM fluorescence similar to DFO (Fig. 8A, B). Next, we measured the expression of ferritin light chain (FTL) using western blotting. FTL is upregulated in the presence of free iron and reduced in expression when iron levels are low (Fujimaki et al., 2019). We observed that BMS536924 caused a reduction in FTL by ~50% in NCI-H522 cells treated for 24 hours (Fig. 8B, C). FTL was dramatically upregulated in cells exposed to 100 μM ferric citrate (Fig. 8B, C). These observations suggest that BMS536924 may block ferroptosis by chelating iron.

Discussion

Mammalian cells use multiple mechanisms to avoid and repair damage to critical macromolecules. ROS created during normal metabolic processes can cause irreversible damage leading cell death. Among the important intracellular targets of ROS, membrane lipids play a key role in a recently described phenomenon called ferroptosis (Li et al., 2020). Peroxidation of membrane lipids leading to cell lysis can occur when antioxidant mechanisms are overwhelmed. Ferroptosis describes a form of peroxidation-driven membrane lysis that occurs in which iron participates in ROS generation and glutathione is needed to lower ROS levels (Li et al., 2020). Inhibitors of cystine import can induce

ferroptosis by limiting intracellular access to cysteine needed for glutathione synthesis (Taylor et al., 2019). Protection of membrane lipids from endogenous ROS is mediated by GPX4, which uses glutathione as a reducing agent to eliminate toxic lipid peroxides. Inhibitors of GPX4 also induce ferroptosis (W. S. Yang et al., 2014). We have recently described a new class of small molecules that inhibit cystine import to induce ferroptosis (Fedorka et al., 2018; Taylor et al., 2019). Consistent with other reports, our compounds are selectively toxic to mesenchymal cancer cells, and cancer stem cells (Taylor et al., 2019).

Despite an explosion of research on ferroptosis, the signaling pathways that modulate this response are incompletely understood. We noticed that ferroptosis did not occur in cells growing in 10% BCS suggesting that some component in serum might modulate this process. Additional studies showed that ferroptosis could occur in serum-free media if compound **1** was added at the same time that serum was removed. However, serum starvation for 24 hours provided partial protection from compound **1**. This suggests that serum starvation may alter cellular physiology to inhibit ferroptosis. In previous work, Gao et al. (2015) found two key components of serum, glutamine and ferritin, were essential for the ferroptosis (Gao et al., 2015). Our experiments involve medium supplemented with glutamine eliminating this amino acid from our interpretations. The fact that ferroptosis still occurs if serum is removed at the time compound **1** is added argues against the possibility that we have removed essential ferroptotic factors, like ferritin. In additional studies we observed that conditioned media enhanced ferroptosis providing evidence that secreted factors may modulate this response. Clearly, the effects of serum factors and associated cellular responses will have complicated effects on ferroptosis.

To better understand the influence of serum on ferroptosis, we carried out a small screen to test the effect of inhibitors of growth factor receptors. We identified BMS536924, an inhibitor of the insulin receptor and the IGF receptor, as a potent inhibitor of ferroptosis. BMS536924 blocked ferroptosis induced by our novel compound as well as RSL3, an inhibitor of GPX4. Simply removing cystine from growth media can also induce ferroptosis. BMS536924 could only partially inhibit ferroptosis induced by cystine removal and we currently do not have an explanation for this effect. The effects of BMS536924 on ferroptosis suggested that insulin signaling might modulate this response. However, IGF1 added exogenously did not affect ferroptosis suggesting instead that BMS536924 had alternative targets to inhibit cell death.

Ferroptosis is dependent on intracellular iron as well as ROS (Dixon et al., 2012). As a consequence, this process can be blocked by iron chelators and antioxidant molecules. Using the stable radical DPPH, we observed that BMS536924 had minimal radical scavenging activity. It is possible that BMS536924 detoxifies specific ROS molecules that we have not measured. Overall, our experiments suggest that BMS536924 is not a general antioxidant. Ferroptosis was originally described as a response to toxic molecules that specifically kill Ras-transformed cells (Yagoda et al., 2007). Thus, it has been proposed that the Ras-MAPK signaling pathway enhances sensitivity to ferroptotic molecules. Studies showing that the MEK inhibitor U0126 blocked ferroptosis appeared to confirm this idea (Yagoda et al., 2007). However, U0126 has subsequently been shown to have radical scavenging activity calling into question the role of Ras-MAPK signaling in ferroptosis (Gao et al., 2015).

BMS536924 was found to inhibit MEK in in vitro reactions (Wittman et al., 2005). However, we found no effect of BMS536924 on ERK phosphorylation suggesting that MEK is likely not important in BMS536924 inhibition of ferroptosis. BMS536924 also inhibits Fak and Lck kinases in vitro (Wittman et al., 2005). Since neither of these kinases have been implicated in ferroptosis, we believe them to be poor candidates to explain the inhibitory activity of BMS536924 on ferroptosis.

Several experiments suggest that BMS536924 may block ferroptosis by chelating iron. First, UV absorbance of BMS536924 was altered when incubated in the presence of iron suggesting a direct association. Second, BMS536924 de-quenched calcein AM fluorescence similar to deferoxamine providing strong evidence for intracellular iron binding. Third, FTL expression was modestly, but reproducibly reduced in cells treated with BMS536924. The reduction of FTL induced by BMS536924 was similar to that observed with the iron chelator deferoxamine (Fujimaki et al., 2019). This effect suggests that these two compounds may have a similar ability to deplete intracellular iron. Together, our observation with UV absorbance, calcein AM fluorescence and western blotting for FTL suggests that BMS536924 acts as an iron chelator. Interestingly, DFO induced a dramatic induction of ERK phosphorylation that was not observed with BMS536924. If this induction is due to iron chelation, the reason that BMS536924-treated cells lack this response is not immediately obvious.

In summary, our analysis of pathways affecting ferroptosis have inadvertently identified a potent inhibitor of the process. BMS536924 was originally described as an inhibitor of insulin signaling. However, in the context of ferroptosis this compound appears instead to act as an iron chelator. These observations should be considered in studies where effects of BMS536924 are instead attributed only to inhibition of insulin signaling.

Supplementary Material

Refer to Web version on PubMed Central for supplementary material.

Acknowledgements.

This project was supported by grant R15CA213185 to L.M.V.T. and R15GM120712 to W.R.T.

ABBREVIATIONS:

ROS	reactive oxygen species
GSH	glutathione
GPX4	glutathione peroxidase 4
SODs	superoxide dismutases
FBS	fetal bovine serum

dFBS	dialyzed FBS
IGF1	Insulin-like growth factor 1
BCS	bovine calf serum
CM	conditioned media
DPPH	2,2-diphenyl-1-(2,4,6-trinitrophenyl)-hydrazyl
FTL	ferritin light chain

References

Brown R, Marshall CJ, Pennie SG, & Hall A (1984). Mechanism of activation of an N-ras gene in the human fibrosarcoma cell line HT1080. EMBO J, 3(6), 1321–1326. Retrieved from https://www.ncbi.nlm.nih.gov/pubmed/6086315 [PubMed: 6086315]

Chen PH, Wu J, Ding CC, Lin CC, Pan S, Bossa N, … Chi JT (2020). Kinome screen of ferroptosis reveals a novel role of ATM in regulating iron metabolism. Cell Death Differ, 27(3), 1008–1022. doi:10.1038/s41418-019-0393-7 [PubMed: 31320750]

Chu B, Kon N, Chen D, Li T, Liu T, Jiang L, … Gu W (2019). ALOX12 is required for p53-mediated tumour suppression through a distinct ferroptosis pathway. Nat Cell Biol, 21(5), 579–591. doi:10.1038/s41556-019-0305-6 [PubMed: 30962574]

Denley A, Cosgrove LJ, Booker GW, Wallace JC, & Forbes BE (2005). Molecular interactions of the IGF system. Cytokine Growth Factor Rev, 16(4–5), 421–439. doi:10.1016/j.cytogfr.2005.04.004 [PubMed: 15936977]

Dixon SJ, Lemberg KM, Lamprecht MR, Skouta R, Zaitsev EM, Gleason CE, … Stockwell BR (2012). Ferroptosis: an iron-dependent form of nonapoptotic cell death. Cell, 149(5), 1060–1072. doi:10.1016/j.cell.2012.03.042 [PubMed: 22632970]

Fedorka SR, So K, Al-Hamashi AA, Gad I, Shah R, Kholodovych V, … Tillekeratne LMV (2018). Small-molecule anticancer agents kill cancer cells by harnessing reactive oxygen species in an iron-dependent manner. Org Biomol Chem, 16(9), 1465–1479. doi:10.1039/c7ob03086j [PubMed: 29411821]

Fujimaki M, Furuya N, Saiki S, Amo T, Imamichi Y, & Hattori N (2019). Iron Supply via NCOA4-Mediated Ferritin Degradation Maintains Mitochondrial Functions. Mol Cell Biol, 39(14). doi:10.1128/MCB.00010-19

Gao M, Monian P, Quadri N, Ramasamy R, & Jiang X (2015). Glutaminolysis and Transferrin Regulate Ferroptosis. Mol Cell, 59(2), 298–308. doi:10.1016/j.molcel.2015.06.011 [PubMed: 26166707]

Kuganesan N, Dlamini S, McDaniel J, Tillekeratne LMV, & Taylor WR (2020). The data that supports the findings of this study are available in the supplementary material of this article.

Lee SM, Lee SB, Prywes R, & Vulpe CD (2015). Iron deficiency upregulates Egr1 expression. Genes Nutr, 10(4), 468. doi:10.1007/s12263-015-0468-0 [PubMed: 25981695]

Li J, Cao F, Yin HL, Huang ZJ, Lin ZT, Mao N, … Wang G (2020). Ferroptosis: past, present and future. Cell Death Dis, 11(2), 88. doi:10.1038/s41419-020-2298-2 [PubMed: 32015325]

Taylor WR, Fedorka SR, Gad I, Shah R, Alqahtani HD, Koranne R, … Tillekeratne LMV (2019). Small-Molecule Ferroptotic Agents with Potential to Selectively Target Cancer Stem Cells. Sci Rep, 9(1), 5926. doi:10.1038/s41598-019-42251-5 [PubMed: 30976078]

Venkatesh D, O'Brien NA, Zandkarimi F, Tong DR, Stokes ME, Dunn DE, … Stockwell BR (2020). MDM2 and MDMX promote ferroptosis by PPARalpha-mediated lipid remodeling. Genes Dev. doi:10.1101/gad.334219.119

Wittman M, Carboni J, Attar R, Balasubramanian B, Balimane P, Brassil P, … Vyas D (2005). Discovery of a (1H-benzoimidazol-2-yl)-1H-pyridin-2-one (BMS-536924) inhibitor of insulin-like

growth factor I receptor kinase with in vivo antitumor activity. J Med Chem, 48(18), 5639–5643. doi:10.1021/jm050392q [PubMed: 16134929]

Wu J, Minikes AM, Gao M, Bian H, Li Y, Stockwell BR, … Jiang X (2019). Intercellular interaction dictates cancer cell ferroptosis via NF2-YAP signalling. Nature, 572(7769), 402–406. doi:10.1038/s41586-019-1426-6 [PubMed: 31341276]

Yagoda N, von Rechenberg M, Zaganjor E, Bauer AJ, Yang WS, Fridman DJ, … Stockwell BR (2007). RAS-RAF-MEK-dependent oxidative cell death involving voltage-dependent anion channels. Nature, 447(7146), 864–868. doi:10.1038/nature05859 [PubMed: 17568748]

Yang WH, & Chi JT (2020). Hippo pathway effectors YAP/TAZ as novel determinants of ferroptosis. Mol Cell Oncol, 7(1), 1699375. doi:10.1080/23723556.2019.1699375 [PubMed: 31993503]

Yang WS, SriRamaratnam R, Welsch ME, Shimada K, Skouta R, Viswanathan VS, … Stockwell BR (2014). Regulation of ferroptotic cancer cell death by GPX4. Cell, 156(1–2), 317–331. doi:10.1016/j.cell.2013.12.010 [PubMed: 24439385]

Zhou Z, Ye TJ, DeCaro E, Buehler B, Stahl Z, Bonavita G, … You M (2020). Intestinal SIRT1 Deficiency Protects Mice from Ethanol-Induced Liver Injury by Mitigating Ferroptosis. Am J Pathol, 190(1), 82–92. doi:10.1016/j.ajpath.2019.09.012 [PubMed: 31610175]

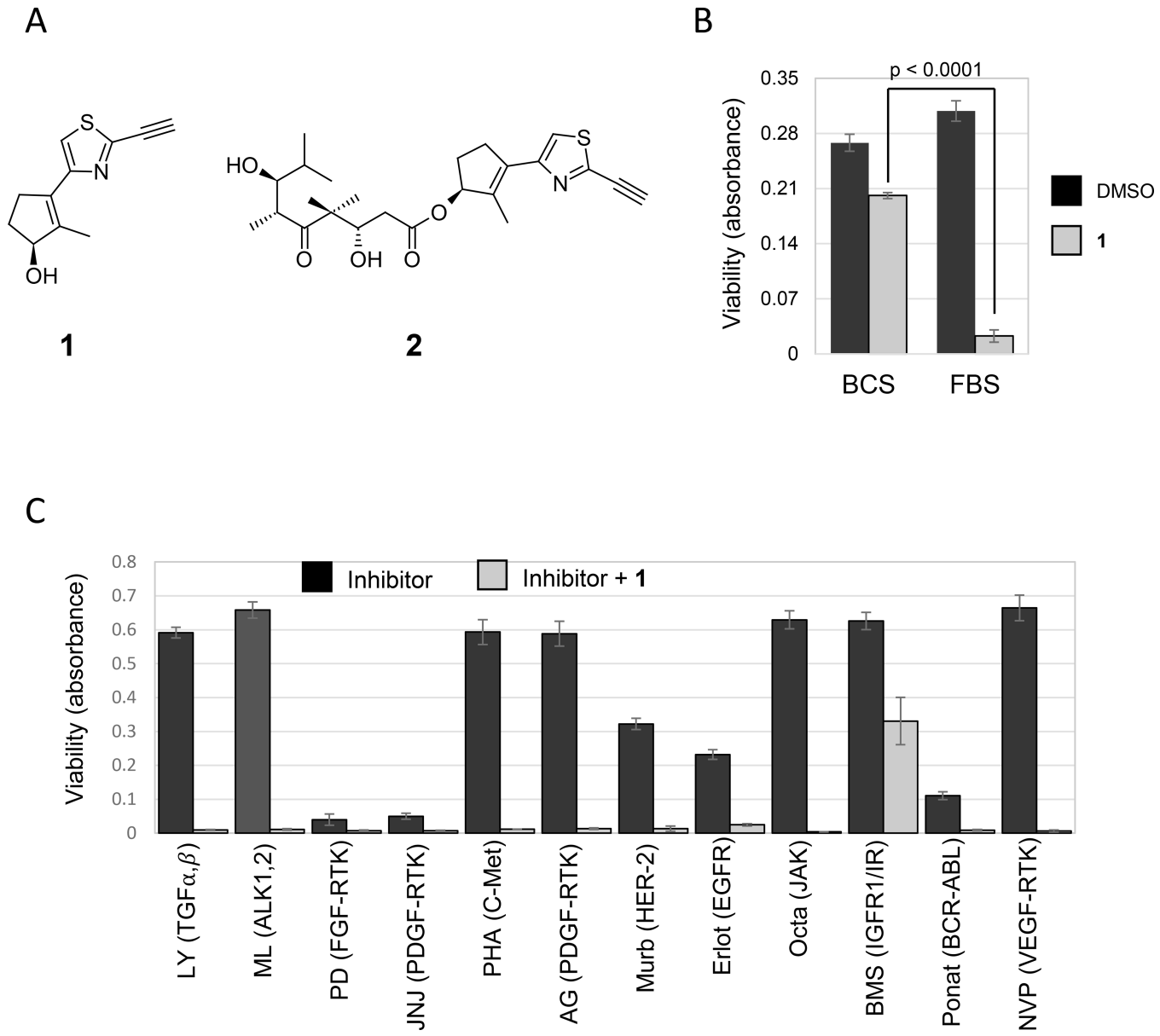

Figure 1.

Effect of Serum and Tyrosine Kinase Inhibitors on Ferroptosis. (A) Compounds used in this study that we have previously described (Fedorka et al., 2018; Taylor et al., 2019). (B) NCI H522 cells robustly undergo ferroptosis in the presence of Fetal bovine serum (FBS) but not Bovine Calf Serum (BCS). Cells were plated in Dulbecco's Modified Eagle Medium (DMEM) containing 10% FBS. Twenty four hours later, the medium was replaced with DMEM containing either 10% FBS or 10% BCS and the cells treated with compound **1** (10 μM) or DMSO (vehicle used to dissolve the compound). (C) Tyrosine kinase inhibitors modulate ferroptosis. NCI H522 cells growing in DMEM+10%FBS were exposed to a panel of receptor tyrosine kinase inhibitors in combination with compound **1**. Compounds were used at the following concentrations: LY 2109761 (2 μM), ML 347 (0.2 μM), PD 173074 (5 μM), JNJ 1098409 (0.1 μM), PHA 665752 (1 μM), AG 1296 (10 μM), Mubritinib (10 μM),

Erlotinib (10 μM), Oclacitib (1 μM), BMS 536924 (1 μM), Ponatinib (1 μM), NVPACC 789 (1 μM) (B and C) Cell survival was determined 72 hours later by methylene blue staining. Viability = absorbance at 668 nm. Bars= mean, error bars=standard deviation, p-value from student t-test (two tailed, unequal variance).

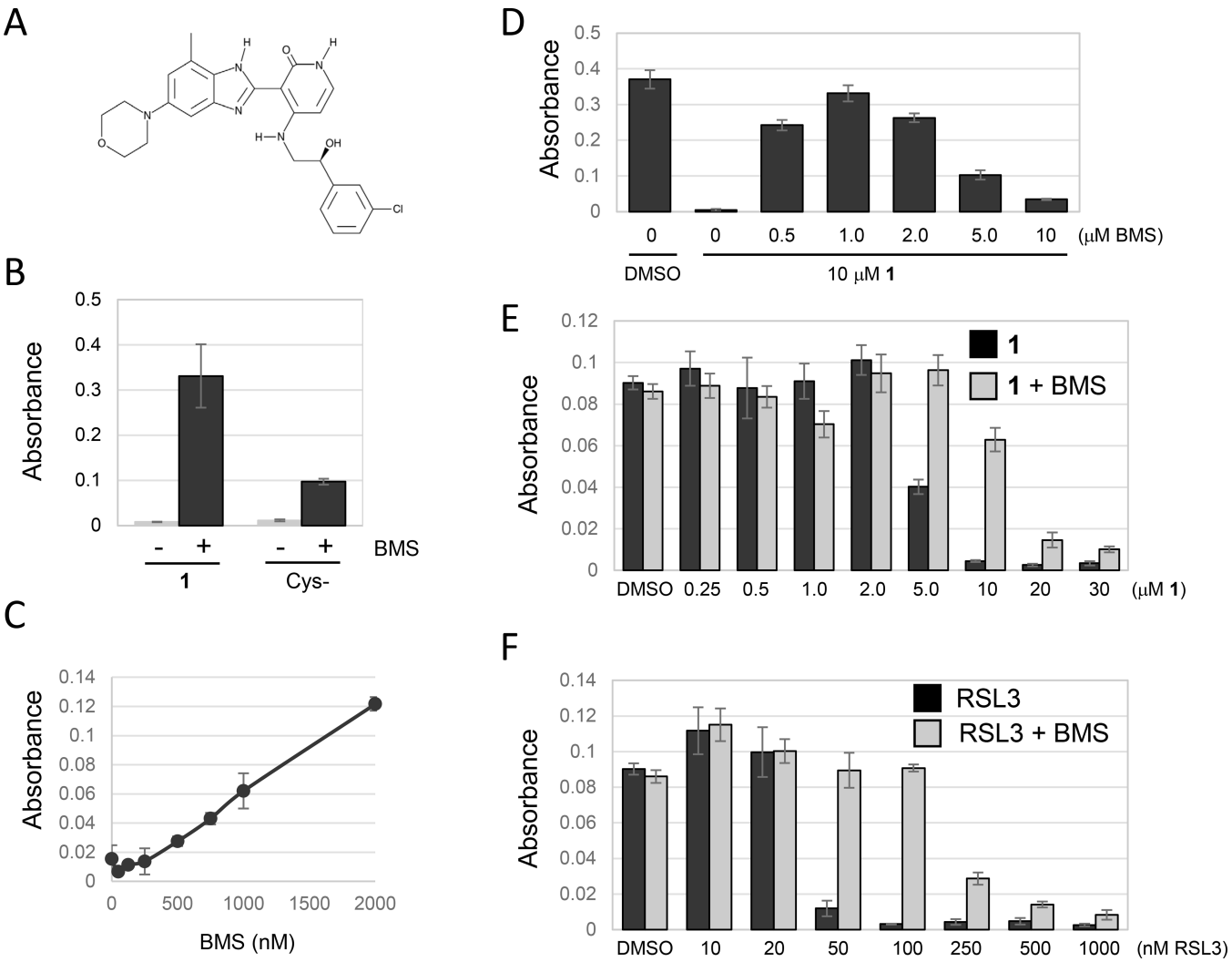

Figure 2.

BMS536924 protects from ferroptotic cell death. Unless otherwise indicated, cell viability was determined using methylene blue staining followed by quantification of absorbance at 668nm. (A) The structure of BMS536924. (B) Effect of BMS536924 on ferroptosis. NCI-H522 cells were plated in DMEM+10% FBS. Twenty four hours later, the media were replaced with cystine-free DMEM containing dialyzed FBS to induce ferroptosis. Alternatively, ferroptosis was induced by leaving cells in DMEM+10% FBS and then exposing to compound **1**. Viability in the presence or absence of BMS536924 (BMS) was assessed 24 hours later. (C) Ferroptosis protection by BMS536924 is dose dependent. Ferroptosis was induced by incubating NCI-H522 cells in cystine-free medium for 24 hours. BMS536924 was added at the concentrations indicated and viability determined. (D) Maximal protection of ferroptosis induced by compound **1** occurs at 1 μM BMS536924. NCI-H522 cells were exposed to the compounds indicated and viability determined 72 hours later. (E and F) BMS536924 rescues from both Type I (compound **1**) and Type II (RSL3) inducers of ferroptosis. NCI H522 cells were exposed to the compounds indicated and viability determined 72 hours later.

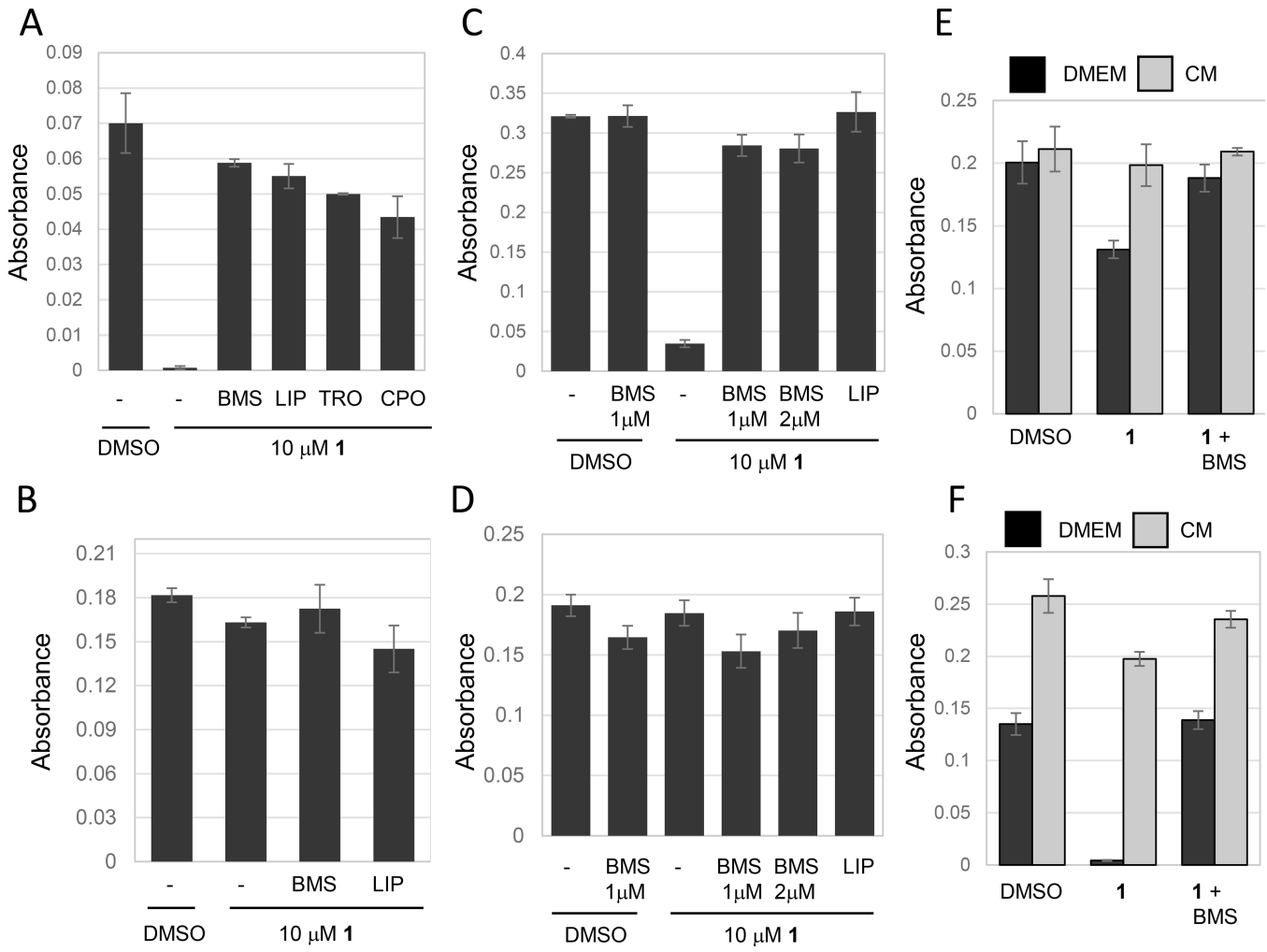

Figure 3.

Serum starvation induces resistance to ferroptosis. Cells were treated as indicated and viability determined using methylene blue 24 hours after drug treatment in all experiments. (A) Removing serum at the time of compound **1** treatment does not block ferroptosis. NCI-H522 cells were plated in DMEM+10% FBS and the next day medium was changed to DMEM without serum. Cells were immediately treated with the compounds indicated. compound **1** was used at 10 μM, BMS536924 at 1 μM, liproxstatin-1 (LIP) at 0.25 μM, trolox (TRO) at 100 μM and ciclopirox (CPO) at 5μM. (B) Serum starvation for 24 hours blocks ferroptosis. NCI- H522 cells were incubated in DMEM without FBS for 24 hours and then treated with compound **1**. Viability was determined 24 hours later. (C and D) Serum starvation also blocks ferroptosis in HT1080. Cells were switched to DMEM without serum either at the time of compound **1** treatment (C), or 24 hours before compound **1** treatment (D) and viability determined. (E and F) Conditioned media enhances ferroptosis. Conditioned medium (CM) was prepared by incubating NCI-H522 cells for either one or two days in the presence of DMEM (no serum). Next, separated plates of NCI-H522 cells were starved for 24 hours in DMEM without serum. Medium was then replaced with 1-day CM (E) or 2-day CM (F). compound **1** as then added and viability determined 24 hours later.

As before, starvation reduces sensitivity to ferroptosis, however ferroptosis returns in cells exposed to 2-day CM.

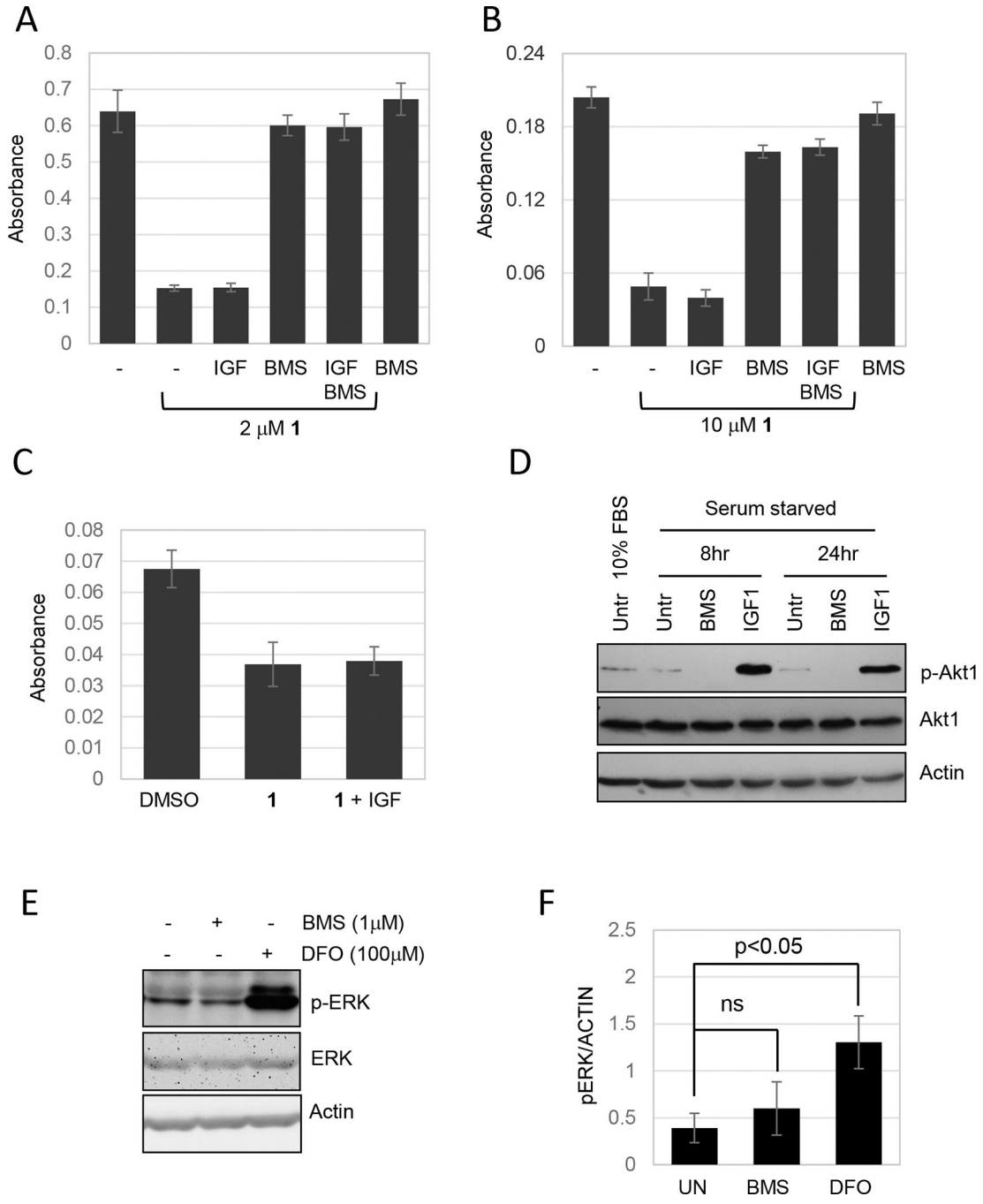

Figure 4.

Effects of BMS536924 on insulin signaling or the ERK pathway does not explain inhibition of ferroptosis. (A, B and C). Cells were exposed to compound **1** in the presence or absence of IGF1 and viability determined by methylene blue staining. (A) NCI H522 and (B) MDA MB 231 cells were treated with compound **1** (as indicated) and/or IGF1 (100 ng/ml) and/or BMS536924 (0.5 μM), 3 days later cell viability was measured. (C) MDA MB 231 cells were starved for 24 hours (DMEM without serum) and then exposed to compound **1** in the presence or absence of IGF1 before analysis of viability. (D) IGF1 induces and BMS536924

blocks Akt1 phosphorylation. MDA MB 231 cells were starved (DMEM without serum) or incubated in DMEM plus 10% FBS for 24 hours. Next, cells were treated with IGF1 (100ng/ml) or BMS536924 (1μM) for 8 or 24 hours. Western blot was probed for p-Akt1, total Akt1 and actin, as a loading control. Akt phosphorylation was measured as a marker for activation of the insulin receptors. (E & F) Effects of BMS536924 on ERK phosphorylation. HT1080 cells were exposed to either BMS536924 or DFO for 24 hours and then analyzed by western blotting with the antibodies indicated. Film images are shown in (E) and pixel intensities from three independent experiments quantified in (F).

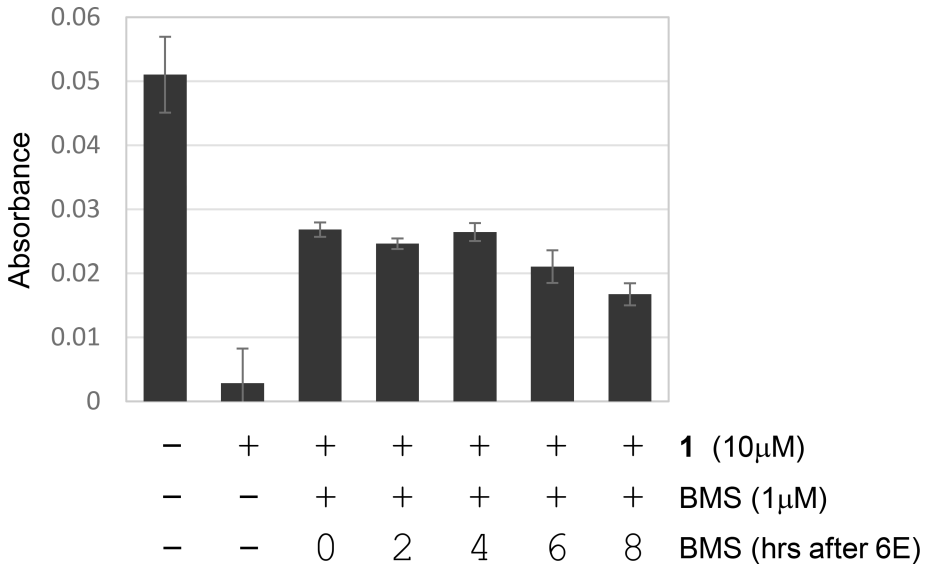

Figure 5. Rapid inhibition of ferroptosis by BMS536924.

NCI-H522 were exposed to compound **1** (10 μM) followed by the delayed addition of BMS536924 (added at 0, 2, 4, 6, 8 hours after compound **1**). Viability was determined 1 day later by methylene blue staining. Protection from ferroptosis was detected even if BMS536924 was added 8 hours after compound **1**, indicated a rapid mode of action.

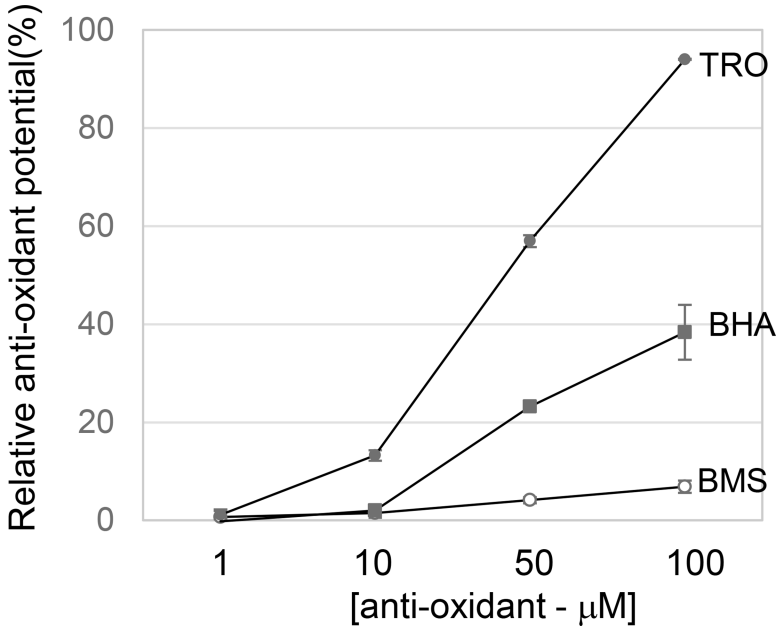

Figure 6. BMS536924 is not a free radical scavenger.

BMS536924, trolox (TRO) or Butylated hydroxyanisole (BHA) were added at the indicated concentrations to a solution containing the colored, stable radical DPPH. Absorbance at 517 nm was assessed. Antioxidant potential was calculated as follows: Raw data were normalized to DMSO, then % reduction was calculated, averaged for anti-oxidant activity and plotted in a line graph.

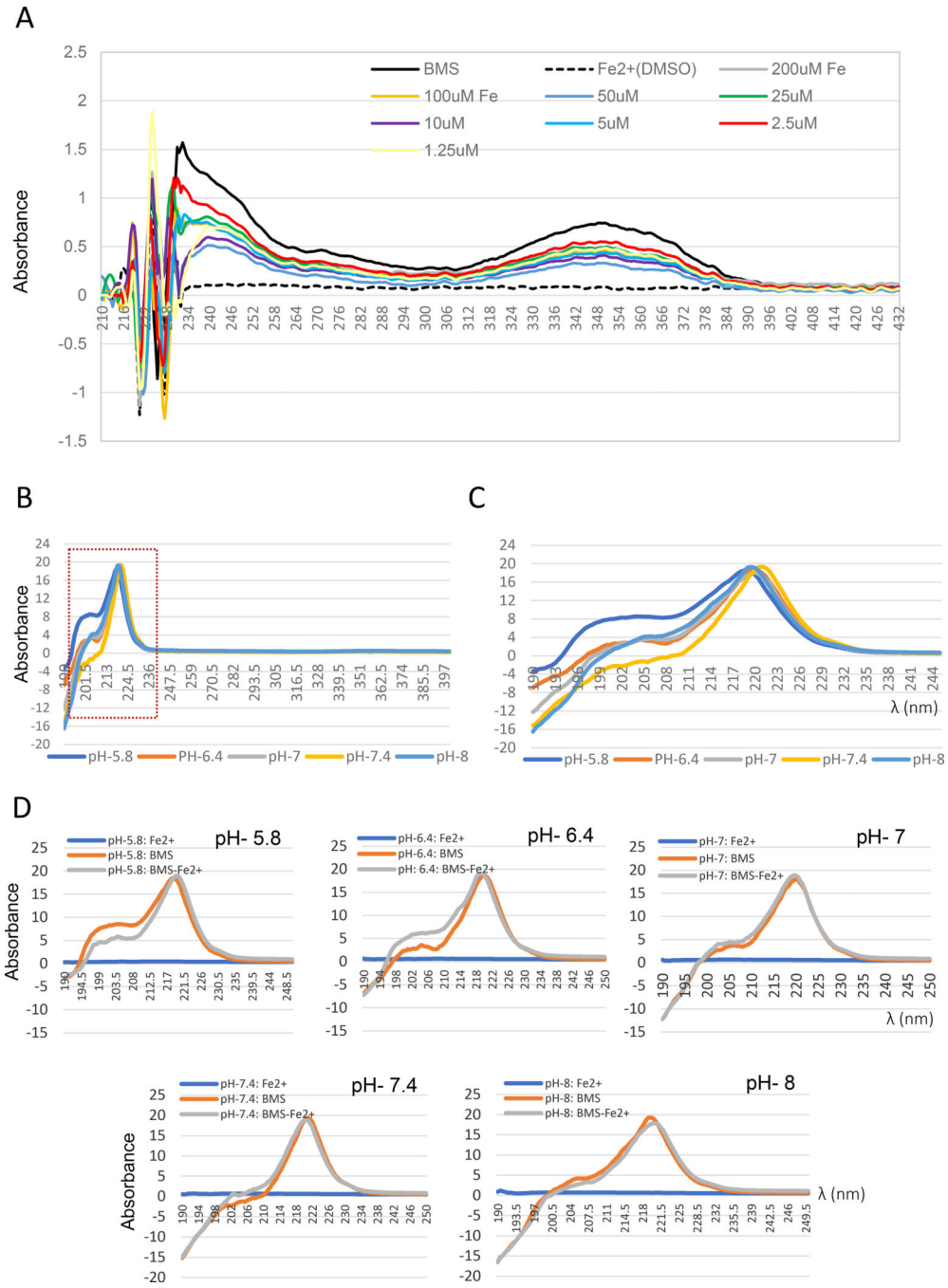

Figure 7. Evidence indicating an interaction of BMS536924 with iron.

(A) UV-Visible absorption spectrum of BMS536924 (100 μM) dissolved in water in the presence of indicated concentrations of iron (2+) in the form of ferrous sulfate. Absorbance from 190 nm to 430 nm is shown. (B-D) Effect of pH on BMS536924/Iron interaction. To test the effect of pH, BMS536924 was dissolved in 0.1M potassium phosphate buffer at pH 5.8, 6.4, 7, 7.4 or 8. (B) UV-Visible absorption spectrum of BMS536924 (100 μM) alone. Potassium phosphate buffer suppressed absorbance at 350 nm whereas absorbance at 220 nm persisted. (C) Effect of pH on BMS536924 absorbance from 190nm to 250nm. (D)

Effect of iron on BMS536924 fluorescence at different pH. BMS536924 (100 μM) was mixed with 100 μM ferrous sulfate (iron 2+) and absorbance from 190 nm to 250 nm is shown.

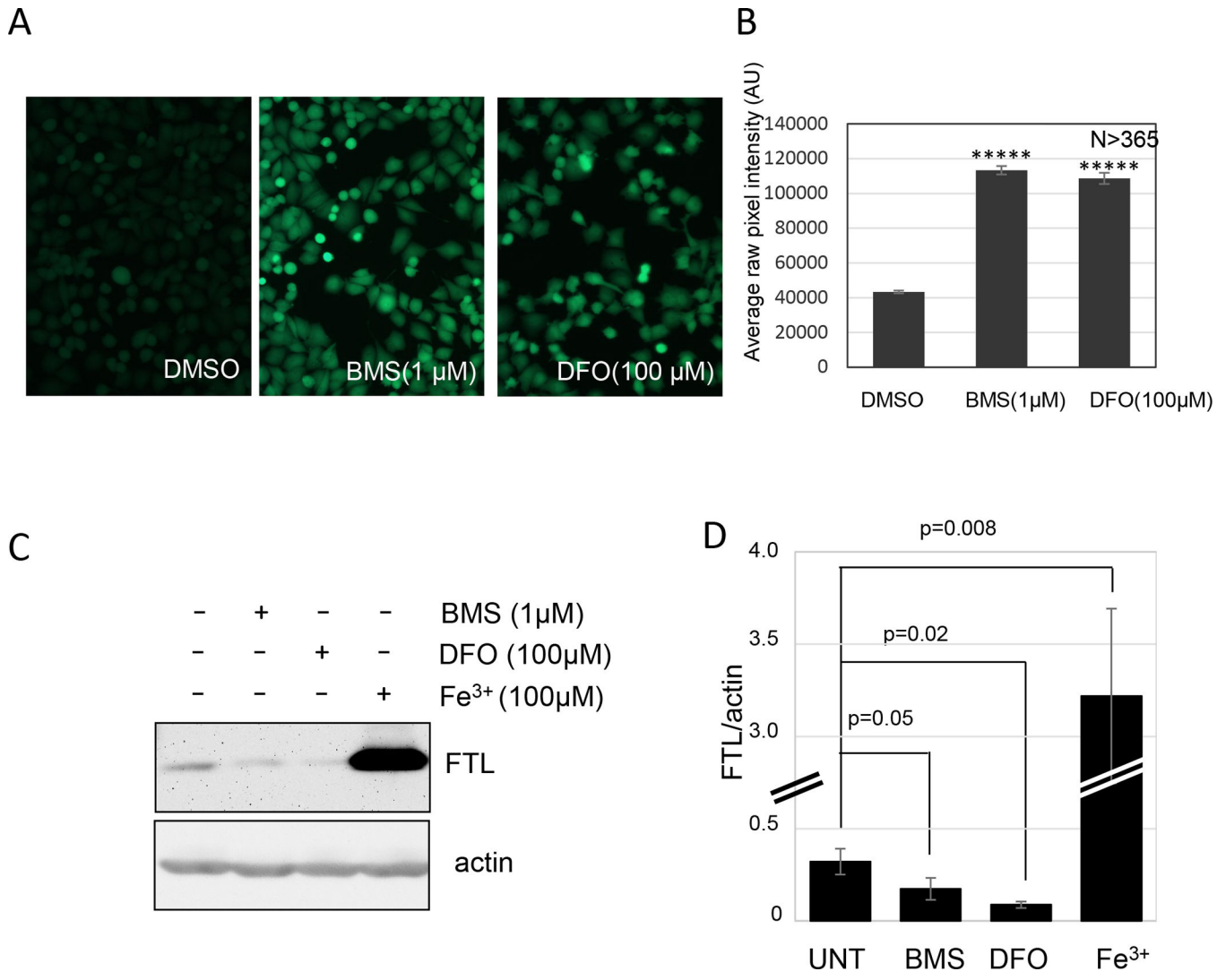

Figure 8.

Iron chelation in cells. (A and B) Effect of BMS536924 on intracellular iron. NCI-H522 cells were exposed to BMS536924 or DFO for 24 hours, and then stained with calcein AM for 15 min. Fluorescent images of live cells shown in (A) were quantified in (B). (C) Effect of BMS536924 and DFO on ferritin light chain (FTL). HT1080 cells were exposed to the compounds indicated for 24 hours and then analyzed by western blotting to measure FTL levels. Images are shown in (D) and pixel intensities from three independent experiments are shown in (C).